doi:10.1093/brain/awq281 Brain 2010: 133; 3676–3684 | 3676

BRAIN
A JOURNAL OF NEUROLOGY

White matter abnormalities in methcathinone abusers with an extrapyramidal syndrome

Ainārs Stepens,[1,*] Charlotte Jane Stagg,[2,3,*] Ardis Platkājis,[4] Marie-Hélène Boudrias,[3] Heidi Johansen-Berg[2,3] and Michael Donaghy[2]

1 Department of Neurology, Riga Stradins University, Riga 1007, Latvia
2 Department of Clinical Neurology, University of Oxford, Oxford, OX3 9DY, UK
3 Centre for Functional Magnetic Resonance Imaging of the Brain (FMRIB), University of Oxford, Oxford OX3 9DU, UK
4 Department of Radiology, Riga Stradins University, Riga 1007, Latvia

*These authors contributed equally to this work.

Correspondence to: Michael Donaghy,
Department of Clinical Neurology,
University of Oxford,
Level 3, West Wing,
John Radcliffe Hospital,
Headington, Oxford,
OX3 9DU,
UK
E-mail: michael.donaghy@clneuro.ox.ac.uk

We examined white matter abnormalities in patients with a distinctive extrapyramidal syndrome due to intravenous methcathinone (ephedrone) abuse. We performed diffusion tensor imaging in 10 patients and 15 age-matched controls to assess white matter structure across the whole brain. Diffuse significant decreases in white matter fractional anisotropy, a diffusion tensor imaging metric reflecting microstructural integrity, occurred in patients compared with controls. In addition, we identified two foci of severe white matter abnormality underlying the right ventral premotor cortex and the medial frontal cortex, two cortical regions involved in higher-level executive control of motor function. Paths connecting different cortical regions with the globus pallidus, the nucleus previously shown to be abnormal on structural imaging in these patients, were generated using probabilistic tractography. The fractional anisotropy within all these tracts was lower in the patient group than in controls. Finally, we tested for a relationship between white matter integrity and clinical outcome. We identified a region within the left corticospinal tract in which lower fractional anisotropy was associated with greater functional deficit, but this region did not show reduced fractional anisotropy in the overall patient group compared to controls. These patients have widespread white matter damage with greatest severity of damage underlying executive motor areas.

Keywords: extrapyramidal syndrome; methcathinone; manganese toxicity; diffusion imaging; white matter tracts

Abbreviations: DTI = diffusion tensor imaging; FSL = Centre for Functional Magnetic Resonance Imaging of the Brain Software Library; SMA = supplementary motor area; TBSS = tract-based spatial statistics; TFCE = threshold-free cluster enhancement; UPDRS = unified Parkinson's disease rating scale

Received April 7, 2010. Revised July 30, 2010. Accepted August 12, 2010. Advance Access publication October 29, 2010

Introduction

A distinctive extrapyramidal syndrome occurs in intravenous methcathinone abusers (Levin, 2005; de Bie *et al.*, 2007; Sanotsky *et al.*, 2007; Sikk *et al.*, 2007; Selikhova *et al.*, 2008; Stepens *et al.*, 2008; Colosimo and Guidi, 2009; Varlibas *et al.*, 2009). Methcathinone is an euphoric stimulant, known as ephedrone in the former USSR, which is manufactured by potassium permanganate oxidation, in the presence of acetic acid, of the ephedrine and pseudoephedrine contained in readily available pharmaceuticals (Zingel *et al.*, 1991; Emmerson and Cisek, 1993). Methcathinone is not isolated in a purified form and intravenous injection exposes users to a high manganese load (Sikk *et al.*, 2007).

Affected users develop a neurological disorder attributed to toxicity from the residual manganese in the injected methcathinone solution. Clinically this involves varying combinations of hypokinesia, dysarthria, dystonia and postural instability (Stepens *et al.*, 2008). A typical patient shows facial impassivity, generally slowed movement, low volume speech, micrographia and a lurching gait on the balls of the feet with absent arm swing. Walking backwards is particularly difficult. Mild executive dysfunction has been detected in some (Selikhova *et al.*, 2008). Unlike Parkinson's disease, there is no rest tremor, lead pipe rigidity, shuffling gait or gait initiation failure. Most patients are unable to work and daily activities are severely restricted, mainly due to gait difficulties and postural instability.

The syndrome is remarkably stereotyped and in active users is associated with a distinctive T_1-weighted MRI signal hyperintensity in the globus pallidus and substantia nigra attributable to manganese deposition; blood manganese levels are markedly elevated (Sikk *et al.*, 2007; Selikhova *et al.*, 2008; Stepens *et al.*, 2008). Although this signal hyperintensity resolves with cessation of methcathinone usage, the clinical syndrome does not improve and is not significantly responsive to antiparkinsonian therapies (Selikhova *et al.*, 2008; Stepens *et al.*, 2008). Furthermore, dopamine transporter single photon emission CT is normal (Selikhova *et al.*, 2008; Sikk *et al.*, 2009) but PET shows widespread, non-uniform, decreased fludeoxyglucose uptake (Sikk *et al.*, 2009). Neuropathological studies of manganese neurotoxicity following occupational or experimental exposure demonstrate cell loss and gliosis in the globus pallidus, particularly the pars interna, with sparing of the substantia nigra pars compacta; Lewy bodies are absent (Olanow *et al.*, 1996; Perl and Olanow, 2007). Manganese-induced neurodegeneration occurs in the frontal cortex of non-human primates associated with a functional deficit in fine motor control (Guilarte *et al.*, 2006, 2008).

Given the distinctive nature of the motor abnormalities in these patients, we investigated whether the syndrome is associated with particular damage to tracts involved in motor control. Although T_1-weighted scans are normal in these patients, apart from the basal ganglia, conventional structural MRI is not always sensitive to diffuse neuronal loss. Diffusion tensor imaging (DTI) is a non-invasive MRI technique sensitive to the self-diffusion of water molecules and provides measures of white matter microstructure. Two DTI metrics, fractional anisotropy and mean diffusivity, are sensitive to subtle white matter abnormalities in various neurological conditions. Decreases in fractional anisotropy reflect a decrease in structure within a tract; factors influencing fractional anisotropy include membrane and myelin integrity and fibre density, but the biological basis of the measure is complex (Beaulieu, 2009). Mean diffusivity is elevated with tissue degeneration and oedema (Assaf, 2008). In Parkinson's disease, decreased fractional anisotropy has been observed in white matter tracts within the frontal lobes (Yoshikawa *et al.*, 2004; Karagulle Kendi *et al.*, 2008; Gattellaro *et al.*, 2009). Changes in mean diffusivity in Parkinson's disease are less consistent across studies; some studies have reported a decrease in mean diffusivity in these areas (Gattellaro *et al.*, 2009), whereas other studies have found mean diffusivity to be normal (Schocke *et al.*, 2002, 2004; Nicoletti *et al.*, 2006; Karagulle Kendi *et al.*, 2008).

We used DTI to investigate forebrain white matter integrity in methcathinone abusers and particularly examined connections between the globus pallidus and cortex.

Materials and methods

Patients

Ten intravenous drug addicts [mean age 40 years (range 30–55), 2 female] who had used methcathinone for an average period of 8 years (range 1–23) and showed the typical extrapyramidal disorder, and 15 controls [mean age 38 years (range 25–56), 2 female] were studied at the University Hospital 'Gailezers', Riga, Latvia in 2008–09. None had a family history of neurological disease, a history of Parkinson's disease or clinical evidence of Lewy body disease. Informed consent was obtained in accordance with the Declaration of Helsinki and ethical approval was granted by the University Hospital, Riga.

Posture, speech and writing were graded as normal, mild, moderate or severe. All patients were rated on the unified Parkinson's disease rating scale, UPDRS (Fahn *et al.*, 1987), a broad measure of parkinsonian symptoms (range 0–176, higher scores indicate more severe disability). As these patients had a pure motor disorder, we utilized the scores from the motor subsection of the UPDRS (section III) for our correlation measures (motor subscore range 0–108; higher scores indicate more severe disability) (Fahn *et al.*, 1987), although it is important to note that this subscore was highly correlated with the total score for these patients, as would be expected in patients with a pure motor disorder.

MRI

Diffusion-weighted magnetic resonance images were acquired on a 1.5 T GE Systems magnetic resonance scanner at the University Hospital 'Gailezers', Riga, Latvia with a maximum gradient strength of 40 mT/m. Echo-planar images of the whole head were acquired (time to repetition = 8500 ms, echo time = 93.9 ms, 27×5-mm-thick axial slices, in-plane resolution 1.0×1.0 mm). The diffusion weighting was isotropically distributed in 25 directions using a b-value of 1000 s/mm^2. One volume with no diffusion weighting was also acquired.

In order for high-resolution tractography to be performed to define pathways of interest between the globus pallidus and cortex, nine healthy controls [mean 27 years (range 22–33), 1 male] were recruited with approval from the Central Oxford Research Ethics Committee and

gave their informed consent in accordance with the Declaration of Helsinki. Diffusion-weighted magnetic resonance images were acquired on a Siemens Sonata 1.5 T scanner at the Oxford Centre for Magnetic Resonance, Oxford, UK, with a maximum gradient strength of 40 mT/m. Three sets of echo-planar images of the whole head were acquired, each with nine volumes with no diffusion weighting (72×2-mm-thick axial slices, giving an isotropic resolution of $2 \times 2 \times 2$ mm). Diffusion weighting was isotropically distributed along 60 directions using a *b*-value of 1000 s/mm^2. This high-resolution dataset was used to define tracts of interest, which were then used to derive quantitative values from age-matched controls and patients; no statistical analysis was performed comparing the controls from the high-resolution dataset with the patient group.

Data analysis

All diffusion data were transformed using affine registration to correct for eddy currents and head motion (Jenkinson *et al.*, 2002) and non-brain tissue was removed (Smith, 2002). The Centre for Functional Magnetic Resonance Imaging of the Brain's diffusion toolbox, part of the Centre for Functional Magnetic Resonance Imaging of the Brain software library (FSL, http://www.fmrib.ox.ac.uk/fsl) (Smith *et al.*, 2004), was used to fit a diffusion tensor model to the data at each voxel. Voxel-wise values of fractional anisotropy and mean diffusivity were then calculated.

Whole brain analysis

Tract-based spatial statistics (TBSS, also part of FSL), a method for voxel-wise statistical comparison of diffusion indices between individuals, was used to test for differences in fractional anisotropy and mean diffusivity between patients and controls across the whole brain white matter (Smith *et al.*, 2006) (see Supplementary material).

To test for group differences in fractional anisotropy or mean diffusivity between patients and controls, we used the randomize program within FSL to carry out permutation-based testing. Statistical thresholding was carried out in two complementary ways: (i) by cluster-based analysis [with corrected cluster ($P < 0.05$) using threshold-free cluster enhancement (TFCE) as implemented within randomize], which is sensitive to spatially extensive areas of significant difference; and (ii) by a voxel-based thresholding approach, which is most sensitive to highly significant differences with small spatial extent. For this voxel-based approach, significant regions were defined by first thresholding the raw *t*-statistic map on the skeleton at $t(23) > 3.76$, giving an (uncorrected) $P < 0.001$. Significant regions were then defined by a cluster extent of >25 mm^3 (equivalent to 5 voxels in native space). This threshold is equivalent to a map-wise false-positive rate of $\alpha < 0.0005$ (estimated using a Monte Carlo procedure as implemented in the AlphaSim program in the analysis of functional neuroimages software package).

For ease of visualization, the results of both the cluster-based and voxel-based analyses were thickened using tbss_fill (within FSL). This thickens the tracts by smoothing with a 3 mm Gaussian kernel, whilst maintaining the maximum statistic values and limiting the extent of the spread to voxels in the white matter (defined as fractional anisotropy >0.2).

We performed a separate within-group analysis of the patient group to test for areas within the white matter skeleton where disability scores correlated with fractional anisotropy or mean diffusivity. Clusters were defined using equivalent thresholding approaches {TFCE (with cluster $P < 0.05$, corrected) and voxel-based thresholding [with $t(9) > 4.29$, giving an (uncorrected) $P < 0.001$, cluster extent of >25 mm^3]}.

Clusters showing significant effects on between-group and within-group analyses with TBSS were used as seed masks for multi-fibre probabilistic tractography (Behrens *et al.*, 2003, 2007) (see Supplementary material) to determine the pathways passing through white matter regions of significant fractional anisotropy or mean diffusivity change. Due to the relatively low resolution of the data collected from the patients and age-matched controls, tractography was performed on higher resolution, isotropic, diffusion weighted images acquired from a separate cohort of healthy controls. It is important to note, however, that these data were not used for any statistical analysis, but only to more accurately define white matter tracts implicated.

Pathways of interest analysis

We had *a priori* hypotheses about involvement of pathways from the globus pallidus in this patient group, given the abnormalities observed in this structure on T_1-weighted MRI. Thus we performed tractography in each high-resolution diffusion dataset to delineate the connections between the globus pallidus and cortical masks, via the thalamus (see Supplementary material), to test specifically for fractional anisotropy or mean diffusivity changes within pathways from the globus pallidus to the cortex. The cortical areas selected were those known to have strong connections with the globus pallidus: primary motor cortex, supplementary motor area (SMA), frontal eye fields, anterior cingulate gyrus, lateral orbital cortex, dorsolateral prefrontal cortex and pre-SMA. Repeated measures ANOVAs were performed to assess the significance of any differences between the groups.

Region of interest analysis of globus pallidus

We wished to investigate differences in mean diffusivity within the globus pallidus itself between patients and controls. To do this, we investigated the average mean diffusivity within the globus pallidus using an anatomical mask (see Supplementary material) for each subject. A two-sample *t*-test was performed to assess the significance of any difference between the groups.

Results

Clinical features

The clinical features of all 10 patients are summarized in Table 1.

MRI

Group differences

A significant increase of 7% in average mean diffusivity within the globus pallidus bilaterally was observed within the patient population compared with the mean value in controls [patients mean diffusivity 8.04 ± 0.09 ($\times 10^{-4}$) (mean $\pm$ SE); controls mean diffusivity 7.49 ± 0.05 ($\times 10^{-4}$); $P < 0.001$].

To investigate global differences between patients and controls in white matter integrity, we tested for differences across the whole white matter skeleton. Overall, patients had a 5% reduction in mean fractional anisotropy compared to controls [patients fractional anisotropy 0.39 ± 0.003 (mean $\pm$ SE); controls fractional anisotropy 0.37 ± 0.007; $t(23) = 2.74$; $P = 0.01$]. Next, we performed a cluster-based (TFCE) analysis within TBSS with a cluster $P = 0.05$ (corrected). TCFE results are fully corrected for

Table 1 Patient characteristics

Patient	Sex	Age	HIV status	Clinical severity							UPDRS		Methcathinone usage
				Gait	Speech	Writing	Rigidity	Tremor	Akinesia	MMSE	Total	Motor	
1	F	42	Negative	Moderate	Mild	Mild	None	None	Moderate	26	36	20	Active
2	M	36	Positive	Severe	Severe	Moderate	None	None	Moderate	30	42	22	Active
3	M	44	AIDS	Severe	Severe	Moderate	None	None	Severe	29	60	35	Former
4	M	40	AIDS	Severe	Moderate	Moderate	None	None	Moderate	29	45	28	Active
5	M	37	AIDS	Moderate	Severe	Severe	None	None	Moderate	29	32	17	Former
6	M	34	Negative	Moderate	Moderate	Moderate	None	None	Moderate	30	48	25	Former
7	M	38	Negative	Severe	Severe	Severe	None	None	Severe	28	55	31	Former
8	M	46	Positive	Moderate	Moderate	Moderate	None	None	Moderate	27	33	19	Active
9	M	55	Negative	Mild	Moderate	Mild	None	None	Moderate	27	42	23	Former
10	F	30	AIDS	Moderate	Moderate	Mild	None	None	Moderate	27	38	22	Active

MMSE = Mini-mental state examination; UPDRS = unified Parkinson's disease rating scale.

family-wise error across the white matter skeleton. Extensive and diffuse areas of decreased fractional anisotropy in patients were observed within the white matter skeleton, particularly in more anterior tracts (Fig. 1A). Within this region, patients had a 15% reduction in mean fractional anisotropy compared to controls (controls 0.48 ± 0.01; patients 0.41 ± 0.01).

We additionally tested for foci of extreme differences in white matter fractional anisotropy between patients and controls using voxel-based thresholding in TBSS. Using this approach, we found two regions of white matter in which the fractional anisotropy was significantly lower in patients than in controls (Table 2, Fig. 1B and C). Both these regions were within the areas of decreased fractional anisotropy in patients demonstrated using TFCE. These clusters were used as seeds for probabilistic tractography, which allowed us to identify these regions as belonging to the anterior corpus callosum connecting the pre-SMA, and to white matter underlying the right ventral premotor cortex (Table 2, Fig. 1B and C). Fractional anisotropy was reduced in these areas by 21% within the region in the anterior corpus callosum and 22% within the region underlying the right ventral premotor cortex. Both these regions were within the areas of decreased fractional anisotropy in patients demonstrated using TFCE.

In the whole brain analysis areas of increased mean diffusivity in the patient group co-distributed with areas of decreased fractional anisotropy (data not shown), but these mean diffusivity increases did not reach statistical significance with either TFCE or voxel-based thresholding.

In addition to whole-brain analysis, we investigated fractional anisotropy and mean diffusivity within known connections between the globus pallidus and distinct cortical areas. There was no main effect of hemisphere [$F(1,24) = 2.59$; $P = 0.12$], therefore mean fractional anisotropy values for the tracts from the two hemispheres were averaged for analyses and a repeated measures ANOVA was performed to test for differences in mean fractional anisotropy within the globus pallidus-cortical tracts between patients and controls. The repeated measures ANOVA revealed a significant main effect of cortical area (primary motor cortex, SMA, frontal eye fields, anterior cingulate gyrus, lateral orbital cortex, dorsolateral prefrontal cortex, pre-SMA) [main effect of area: $F(6,138) = 1051$, $P < 0.001$] and a significant overall difference in mean fractional anisotropy between patient and control groups [main effect of group: $F(1,23) = 6.61$, $P = 0.01$], as well as a significant interaction between area and group [interaction of area × group: $F(6,138) = 6.00$, $P < 0.001$]. *Post hoc* *t*-tests demonstrated a reduction in fractional anisotropy in patients compared to controls within each of these tracts (Table 3).

A repeated measures ANOVA was performed to test for differences in average mean diffusivity within the globus pallidus-cortical tracts between controls. There was a significant main effect of cortical area (primary motor cortex, SMA, frontal eye fields, anterior cingulate gyrus, lateral orbital cortex, dorsolateral prefrontal cortex, pre-SMA) [$F(6,138) = 529$, $P < 0.002$], a significant overall difference in average mean diffusivity between the patient and control groups [$F(1,23) = 5742$, $P < 0.001$] and a significant interaction between area and group [$F(6,138) = 3.39$, $P = 0.004$]. *Post hoc* *t*-tests demonstrated a trend towards an increase in mean diffusivity in the patient group in each of these tracts, though this did not reach significance.

Correlations with disability

Clinical scores were correlated with white matter fractional anisotropy within the patient population. No significant clusters were identified using TFCE, but using voxel-based correction there was a significant correlation between the UPDRS motor subscore and fractional anisotropy in one region (Table 2, Fig. 2A), such that patients with a higher motor subscore (i.e. those with greater disability) had lower fractional anisotropy in this region (Fig. 2C). Probabilistic tractography allowed us to identify this region as belonging to the left corticospinal tract (Fig. 2B). Motor subscore and total UPDRS score were highly correlated within this patient group ($r = 0.97$, $P < 0.001$) and the same region showed a significant correlation between total UPDRS score and fractional anisotropy. This region did not appear to have reduced fractional anisotropy in the patient group as a whole in our analysis of between-group differences (Fig. 1A). Consistent with this, a region of interest analysis on this cluster showed that the fractional anisotropy within this region was not significantly lower in patients than in controls (Fig. 2D).

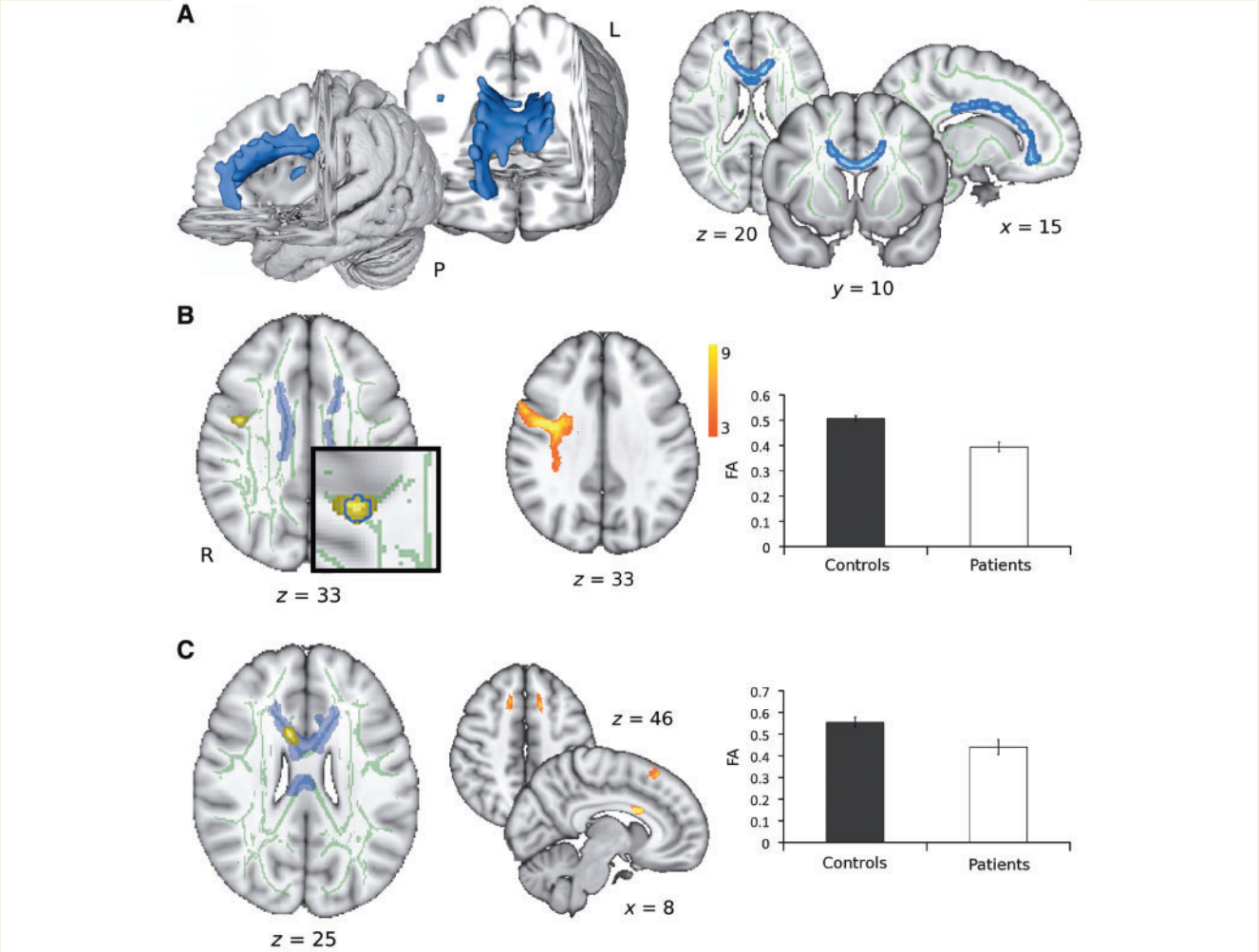

Figure 1 Group differences in fractional anisotropy between patients and controls. (**A**) Blue regions indicate areas showing a significant reduction in fractional anisotropy in patients compared to controls in a cluster-based analysis (significant clusters have been thickened for ease of visualization) (TFCE; corrected $P < 0.05$). Widespread abnormalities are observed in white matter tracts within the central regions of the brain, more peripheral tracts are relatively unaffected. (**B** and **C**) Areas showing decreased fractional anisotropy in patients compared to controls using voxel-based thresholding. The first column shows regions of significant reduction in fractional anisotropy in yellow (significant clusters have been thickened for ease of visualization) [$t > 3.76$; $P < 0.001$ (uncorrected); cluster extent > 25 mm^3]. The mean fractional anisotropy skeleton is shown in green and the areas of significant difference illustrated in **A** are shown in blue. The middle column shows the paths (derived using high-resolution diffusion data from healthy volunteers) originating from the clusters of significant difference shown in the first column where the colour coding reflects the proportion of the population in which a tract is present. Tracts have been thresholded to show only those present in ≥ 3 subjects. The third column shows the mean fractional anisotropy in patients and controls within the significant clusters. FA = fractional anisotropy; L = lateral; P = posterior.

Table 2 White matter regions in which fractional anisotropy values (A) were significantly lower in patients than controls, and (B) correlated with clinical score

Cluster location	Max *t*-statistic	Size in mm^3	Centre of gravity		
			x	*y*	*z*
(A) Patients versus controls					
Under right ventral premotor cortex	6.35	31	43	−2	33
Right corpus callosum	4.63	34	11	13	25
(B) Correlation with UPDRS (motor subscore)					
Left corticospinal tract	5.79	47	−25	−25	37

A similar region was identified in the right corticospinal tract, but the cluster extent (15 mm^3) did not reach our significance threshold (>25 mm^3). Analysis of mean diffusivity demonstrated no areas of significant correlation with UPDRS scores.

Table 3 Summary of mean fractional anisotropy within globus pallidus–cortical tracts used for the pathways of interest analysis

Region	Mean fractional anisotropy		*P*-value
	Controls	Patients	
Primary motor cortex	0.29 ± 0.002	0.28 ± 0.006	0.02
SMA	0.31 ± 0.002	0.29 ± 0.006	0.02
Frontal eye fields	0.31 ± 0.002	0.30 ± 0.006	0.02
Anterior cingulate gyrus	0.30 ± 0.003	0.27 ± 0.007	0.01
Lateral orbital cortex	0.27 ± 0.002	0.26 ± 0.005	0.02
Dorsolateral prefrontal cortex	0.29 ± 0.002	0.27 ± 0.006	0.02
Pre-SMA	0.31 ± 0.002	0.29 ± 0.006	0.02

The mean fractional anisotropy within these pathways was reduced in the patient group compared to the controls (mean ± SE). *Post hoc t*-tests were performed to assess the significance of this difference. The resulting *P*-value is shown in Column 4. SMA = supplementary motor area.

We found no correlations between clinical score and either fractional anisotropy or mean diffusivity within the globus pallidus-cortical tracts.

Discussion

We identified white matter abnormalities in methcathinone abusers with an extrapyramidal syndrome. Evidence for diffuse white matter change was reflected by reductions in fractional anisotropy within the central white matter of the patient group. In addition, we found focally severe reductions in fractional anisotropy in the patient group—specifically in areas underlying the right ventral premotor cortex and the medial prefrontal cortex. A correlation between clinical severity and white matter integrity was demonstrated within the left corticospinal tract, in a region that appears to be relatively spared in the group as a whole.

Given the nature of the underlying toxicity in these patients, widespread damage to the white matter tracts, as evidenced by reduction in fractional anisotropy, might have been expected.

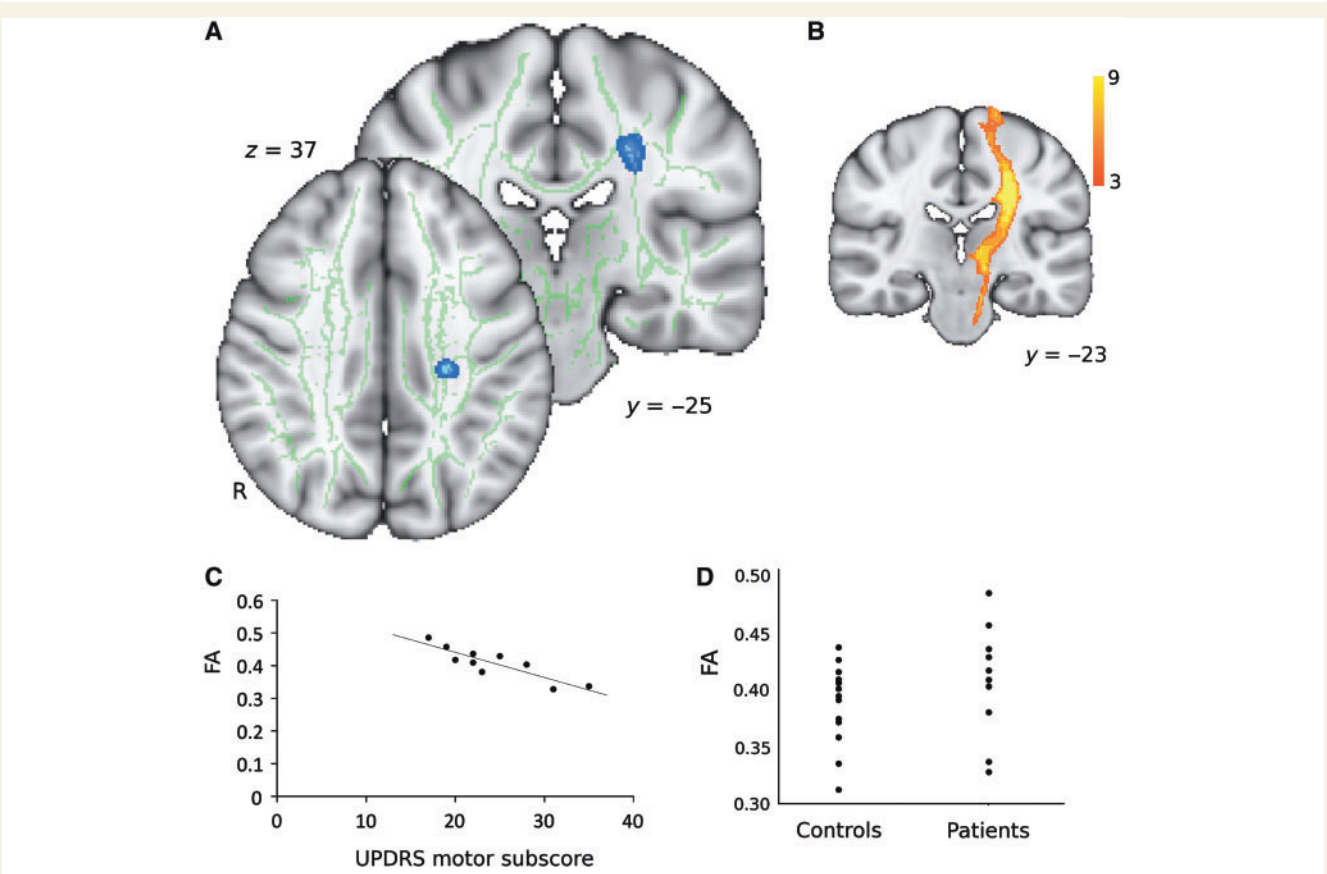

Figure 2 Correlations with clinical score. (**A**) The blue region indicates an area showing a significant correlation between UPDRS motor subscore and fractional anisotropy using voxel-based thresholding [$t > 4.78$, $P < 0.001$ (uncorrected), cluster extent >25 mm^3]. (**B**) The results of probabilistic tractography using this region as a seed mask in high-resolution data, demonstrating it lies within the left corticospinal tract, where the colour coding reflects the proportion of the population in which a tract is present. Tracts have been thresholded to show only those present in at least three out of nine subjects. (**C**) Correlation between UPDRS motor subscore and fractional anisotropy (FA) within this region. (**D**) Range of FA within this region in patients and controls (points represent individual subjects).

More noteworthy is the demonstration of focal regions of substantial reduction in fractional anisotropy. The clinical features of these patients point to a disorder of higher-level motor programming. They have notable difficulty with backwards motion, tend to fall if walking backwards, sit by falling backwards and recover poorly on backwards displacement. An early symptom is difficulty in getting out of cars and one patient had extreme difficulty propelling his wheelchair backwards using his hands, despite easily moving it forwards (Stepens *et al.*, 2008). This pattern of motor deficits resembles executive dysfunction displayed by patients with prefrontal lesions who typically have difficulties in inhibiting a prepotent response (Mostofsky and Simmonds, 2008). The regions of the medial and inferior lateral frontal cortex implicated here are involved in circumstances where an initial response must be suppressed to perform a different required action (Aron *et al.,* 2004; Nachev *et al.*, 2007; Mostofsky and Simmonds, 2008; Mars *et al.*, 2009; Buch *et al.*, 2010) and individual differences in the microstructure of white matter pathways that interconnect with the pre-SMA and ventral premotor cortex correlate with physiological measures of response inhibition, even in healthy subjects (Mars *et al.,* 2009; Buch *et al.,* 2010). The difficulty these patients have in moving backwards may therefore result from an inability to suppress the primary action of walking forwards.

T_1-weighted structural MRI reveals the globus pallidus as the primary site of manganese deposition in these patients (Stepens *et al.*, 2008). We have demonstrated increased mean diffusivity in this area, unlike Parkinson's disease (Chan *et al.*, 2007), suggesting loss of microstructural integrity specifically in our patient group. The anatomical connectivity of the globus pallidus involves basal ganglia cortical loops with areas of prefrontal, premotor and motor cortex (Middleton and Strick, 2000) and DTI confirms similar connections in humans (Draganski *et al.*, 2008). We used tractography to test specifically for white matter abnormalities within globus pallidus–cortical connections and demonstrated widespread damage across all tracts. Although the ANOVA revealed an interaction suggesting the globus pallidus–cortical connections are differentially affected by the disease process, our *post hoc t*-tests detected a decreased fractional anisotropy in patients in all tracts. There are a number of reasons that an increase in mean diffusivity and a decrease in fractional anisotropy might be observed in the globus pallidus–cortical pathways. It might be that manganese toxicity leads to a more widespread pattern of neuronal damage than that inferred from conventional MRI. Alternatively, it might be that there is a decrease in fractional anisotropy in these tracts as a secondary trans-synaptic consequence of damage to the globus pallidus, and therefore a decrease in tract integrity is observed secondary to a decrease in the pre-synaptic globus pallidus–thalamic connections.

By contrast to the globus pallidus–cortical connections, the corticospinal tracts appear to be relatively spared, in keeping with the lack of pyramidal signs in these patients. In combination with the result of the whole brain analysis, this anatomical pattern reinforces the clinical notion of a higher-level motor programming disorder. However, despite the relative sparing of the corticospinal tracts, we also demonstrated a significant correlation between fractional anisotropy within the left corticospinal tract and clinical score in the patients. This may suggest that pre-existing variation in this pathway influences motor function in patients, reminiscent of correlations between fractional anisotropy and performance described in healthy volunteers (Johansen-Berg *et al.,* 2007).

Tractography has not been used previously to investigate manganese toxicity. DTI has been used to investigate Parkinson's disease and parkinsonian syndromes, showing decreased fractional anisotropy outside the basal ganglia within the genu of the corpus callosum and the superior longitudinal fasciculus, and within fontal lobe areas, premotor areas and the cingulum (Yoshikawa *et al.*, 2004; Karagulle Kendi *et al.*, 2008; Gattellaro *et al.*, 2009). Although two of these previous studies in non-demented patients report decreased fractional anisotropy in widespread regions of frontal white matter that include locations demonstrated here (Karagulle Kendi *et al.*, 2008; Gattellaro *et al.*, 2009), it is important to reiterate that the extrapyramidal syndrome in methcathinone abusers differs markedly from that of Parkinson's disease.

The focal white matter abnormality underlying the ventral premotor cortex was only detected in the right hemisphere, even after relaxing the statistical thresholding ($P < 0.05$ uncorrected, voxel extent $>25\,mm^3$; data not shown). There is a known functional laterality within the motor system in that the left premotor cortex is dominant for selection of motor actions (Cavina-Pratesi *et al.*, 2006). It is not clear why the right ventral premotor cortex is more sensitive in this context, given that the pathology, conventional magnetic resonance changes and clinical disorder are symmetric. However, it is interesting to note that a previous study on Parkinson's disease reported right lateralized changes in white matter fractional anisotropy in a location encompassing this region (Karagulle Kendi *et al.*, 2008).

There is a complex neurobiological basis for the fractional anisotropy measure used here. Fractional anisotropy is modulated by factors such as myelination, membrane integrity or axonal packing density (Beaulieu, 2009). In the context of toxin-induced neuronal loss, the decreases are likely to reflect decreased axonal packing density; however this cannot be proven definitively using this technique. Additionally, possible compensatory adaptive changes in myelination, for example, cannot be excluded (Tanaka *et al.*, 2003). More complex acquisition and analysis of diffusion data may allow modelling of specific microstructural features such as axon diameter (Assaf *et al.*, 2008).

Of our six HIV-positive patients, four had AIDS. We confirmed that HIV status has no effect on differences between patients and controls (data not shown). Although these conditions can lead to white matter abnormalities, a recent study demonstrated no difference in fractional anisotropy between HIV-positive patients and healthy controls (Gongvatana *et al.*, 2009). Although decreases in fractional anisotropy have been observed in patients with AIDS they mainly relate to dementia (Mirsattari *et al.,* 1998).

Methodological limitations

Our studied patient population is relatively small, a common limitation of imaging studies in rare disorders. Despite the small group sizes, we detected consistent changes to guide future studies on

larger groups. In the current study we were unable to test quantitatively for grey matter changes due to the limited resolution of T_1-weighted images. Future studies should investigate disease-related changes in the grey matter areas that interconnect with the white matter regions indentified here. The resolution of the DTI data for patients and age-matched controls was also relatively low and this may have reduced our sensitivity to focal effects and limited the accuracy of cross-subject alignment. Registration accuracy was checked for all subjects and we de-projected significant clusters back into native DTI space for each individual to confirm that skeleton voxels were indeed projected from the white matter in all cases.

Conclusion

We have demonstrated widespread white matter abnormalities in patients with a manganese-induced extrapyramidal syndrome. Particular abnormalities were noted within white matter underlying two regions known to be involved in higher-level motor processes, which may explain the stereotypic motor impairment of these patients. The detection of these abnormalities outside areas known to be connected directly to the globus pallidus suggests a more widespread neuronal pathology than previously demonstrated by conventional imaging techniques, thereby extending our understanding of the anatomical basis of this disorder.

Funding

National Institute for Health Research Oxford Biomedical Research Centre (to H.J.B. and C.J.S.); the Wellcome Trust (to H.J.B.) and the European Social Fund (to A.S.).

Supplementary material

Supplementary material is available at *Brain* online.

References

Aron AR, Robbins TW, Poldrack RA. Inhibition and the right inferior frontal cortex. Trends Cogn Sci 2004; 8: 170–7.

Assaf Y. Can we use diffusion MRI as a bio-marker of neurodegenerative processes? BioEssays 2008; 30: 1235–45.

Assaf Y, Blumenfeld-Katzir T, Yovel Y, Basser PJ. Axcaliber: a method for measuring axon diameter distribution from diffusion MRI. Magn Reson Med 2008; 59: 1347–54.

Beaulieu C. The biological basis of diffusion anisotropy. In: Johansen-Berg H, Behrens TEJ, editors. Diffusion MRI: From quantitative measurement to in-vivo neuroanatomy. London: Elsevier; 2009. p. 105–26.

Behrens T, Johansen-Berg H, Jbabdi S, MFS R, Woolrich M. Probabilistic diffusion tractography with muleipl fibre orientations. What can we gain? Neuroimage 2007; 23: 144–55.

Behrens T, Woolrich M, Jenkinson M, Johansen-Berg H, Nunes R, Clare S, et al. Characterization and propogation of uncertainty in diffusion-weighted MR imaging. Magn Reson Med 2003; 50: 1077–88.

Buch ER, Mars RB, Boorman ED, Rushworth MFS. A network centered on ventral premotor cortex exerts both facilitatory and inhibitory control over primary motor cortex during action peprogramming. J Neurosci 2010; 30: 1395–401.

Cavina-Pratesi C, Valyear KF, Culham JC, Kohler S, Obhi SS, Marzi CA, et al. Dissociating arbitrary stimulus-response mapping from movement planning during preparatory period: evidence from event-related functional magnetic resonance imaging. J Neurosci 2006; 26: 2704–13.

Chan L-L, Rumpel H, Yap K, Lee E, Loo H-V, Ho G-L, et al. Case control study of diffusion tensor imaging in Parkinson's Disease. J Neurol Neurosurg and Psychiatry 2007; 78: 1383–6.

Colosimo C, Guidi M. Parkinsonism due to ephedrone neurotoxicity: a case report. Eur J Neurol 2009; 16: e114–5.

de Bie R, Gladsonte R, Strafella A, Ko J, Lang A. Manganese-induced Parkinsonism associated with methcathinone (ephedrone) abuse. Arch Neurol 2007; 64: 886–9.

Draganski B, Kherif F, Klappel S, Cook P, Alexander D, Parker G, et al. Evidence for segregated and integrative connectivity patterns in the human basal ganglia. J Neurosci 2008; 28: 7143–52.

Emmerson T, Cisek J. Methcathinone: a russian designer amphetamine infiltrates the rural midwest. Ann Emerg Med 1993; 22: 1897–903.

Fahn S, Marsden C, Calne DB. Recent developments in Parkinson's Disease. Florham Park, NJ: Macmillan Health Care Information; 1987.

Gattellaro G, Minati L, Grisoli M, Mariani C, Carella F, Osio M, et al. White matter involvement in idiopathic Parkinson disease: a diffusion tensor imaging study. Am J Neuroradiol 2009; 30: 1222–6.

Gongvatana A, Schweinsburg B, Taylor M, Theilmann R, Letendre S, Alhassoon O, et al. White matter tract injury and cognitive impairment in human immunodeficiency virus infected individuals. J Neurovirol 2009; 15: 187–95.

Guilarte T, Burton N, Verina T, Prabhu V, Becker K, Syversen T, et al. Increased APLP1 expression and neurodegeneration in the frontal cortex of manganese-exposed non-human primates. J Neurochem 2008; 105: 1948–59.

Guilarte T, McGlothan J, Degaonkar M, Chen M-K, Barker P, Syversen T, et al. Evidence for cortical dysfunction and widespread manganese accumulation in the nonhuman primate brain following chronic manganese exposure: a 1H-MRS and MRI study. Toxicol Sci 2006; 94: 351–8.

Jenkinson M, Bannister P, Brady J, Smith S. Improved optimisation for the robust and accurate linear registration and motion correction of brain images. Neuroimage 2002; 17: 825–41.

Johansen-Berg H, Della-Maggiore V, Behrens TEJ, Smith SM, Paus T. Integrity of white matter in the corpus callosum correlates with bimanual co-ordination skills. Neuroimage 2007; 36: T16–21.

Karagulle Kendi AT, Lehericy S, Luciana M, Ugurbil K, Tuite P. Altered diffusion in the frontal lobe in Parkinson disease. Am J Neuroradiol 2008; 29: 501–5.

Levin O. "Ephedron" encephalopathy. Zh Nevrol Psikhitr Im S S Korsakova 2005; 105: 12–20 (in Russian).

Mars R, Klein M, Neubert F, Olivier E, Buch E, Boorman E, et al. Short-latency influence of medial frontal cortex on primary motor cortex during action selection under conflict. J Neurosci 2009; 29: 6926–31.

Middleton FA, Strick PL. Basal ganglia output and cognition: evidence from anatomical, behavioral, and clinical studies. Brain Cognition 2000; 42: 183–200.

Mirsattari SM, Power C, Nath A. Parkinsonism with HIV infection. Mov Dis 1998; 13: 684–9.

Mostofsky SH, Simmonds DJ. Response inhibition and response selection: two sides of the same coin. J Cogn Neurosci 2008; 20: 751–61.

Nachev P, Wydell H, O'Neill K, Husaim M, Kennard C. The role of the pre-supplementary motor area in the control of action. Neuroimage 2007; 36: 115–63.

Nicoletti G, Lodi R, Condino F, Tonon C, Fera F, Malucelli E, et al. Apparent diffusion coefficient measurements of the middle cerebellar peduncle differentiate the Parkinson variant of MSA from Parkinson's disease and progressive supranuclear palsy. Brain 2006; 129: 2679–87.

Olanow CW, Good PF, Shinotoh H, Hewitt KA, Vingerhoets F, Snow BJ, et al. Manganese intoxication in the rhesus monkey: a clinical, imaging, pathologic, and biochemical study. Neurology 1996; 46: 492–8.

Perl DP, Olanow CW. The neuropathology of manganese-induced Parkinsonism. J Neuropath Exp Neurol 2007; 66: 675–82.

Sanotsky Y, Lesyk R, Fedoryshyn L, Komnatska I, Matviyenko Y, Fahn S. Manganic encephalopathy due to "ephedrone" abuse. Movement Dis 2007; 22: 1337–43.

Schocke MF, Seppi K, Esterhammer R, Kremser C, Jaschke W, Poewe W, et al. Diffusion-weighted MRI differentiates the Parkinson variant of multiple system atrophy from PD. Neurology 2002; 58: 575–80.

Schocke MF, Seppi K, Esterhammer R, Kremser C, Mair KJ, Czermak BV, et al. Trace of diffusion tensor differentiates the Parkinson variant of multiple system atrophy and Parkinson's disease. Neuroimage 2004; 21: 1443–51.

Selikhova M, Fedoryshyn L, Matviyenko Y, Komnatska I, Kyrylchuk M, Krolicki L, et al. Parkinsonism and dystonia caused by the illicit use of ephedrone-A longitudinal study. Movement Dis 2008; 23: 2224–31.

Sikk K, Taba P, Haldre S, Bergquist J, Nyholm D, Askmark H, et al. Clinical, neuroimaging and neurophysiological features in addicts with manganese-ephedrone exposure. Acta Neurol Scand 2010; 121: 237–43.

Sikk K, Taba P, Haldre S, Bergquist J, Nyholm D, Zjablov G, et al. Irreversible motor impairment in young addicts - epehdrone, manganism or both? Acta Neurol Scand 2007; 115: 385–9.

Smith SM. Fast, Robust automated briain extraction. Hum Brain Mapp 2002; 17: 143–55.

Smith SM, Jenkinson M, Johansen-Berg H, Rueckert D, Nichols TE, Mackay CE, et al. Tract-based spatial statistics: voxelwise analysis of multi-subject diffusion data. Neuroimage 2006; 31: 1487–505.

Smith SM, Jenkinson M, Woolrich MW, Beckmann CF, Behrens T, Johansen-Berg H, et al. Advances in functional and structural MR image analysis and implementation as FSL. Neuroimage 2004; 23: S208–19.

Stepens A, Logina I, Liguts V, Aldins P, Eksteina I, Platkajis A, et al. A Parkinsonian syndrome in methcathinone users and the role of manganese. N Engl J Med 2008; 358: 1009–17.

Tanaka K, Nogawa S, Suzuki S, Dembo T, Kosakai A. Upregulation of oligodendrocyte progenitor cells associated with restoration of mature oligodendrocytes and myelination in peri-infarct area in the rat brain. Brain Res 2003; 989: 172–9.

Varlibas F, Delipoyraz I, Yuksel G, Filiz G, Tireli H, Gecim N. Neurotoxicity following chronic intravenous use of "Russion cocktail" . Clin Toxicol 2009; 47: 157–60.

Yoshikawa K, Nakata Y, Yamada K, Nakagawa M. Early pathological changes in the parkinsonian brain demonstrated by diffusion tensor MRI. J Neurol Neurosurg Psychiatry 2004; 75: 481–4.

Zingel K, Dovensky W, Crossman A, Allen A. Ephedrone 2-methylamino-1-phenylpropane-1-one (Jeff). J Forensic Sci 1991; 36: 915–20.